

Numerical Calculation and Analysis of Automobile Aerodynamic Noise Based on Large Eddy Simulation

J. H. Tang^{†*}, Y. Y. Zuo[‡], S. Y. Bei[†], & K. Y. Wang^{†‡}

[†]School of Automotive and Traffic Engineering, Jiangsu University of Technology, Changzhou 213001, China,

*Email: wkuiy@126.com

[‡]School of Automotive and Traffic Engineering, Jiangsu University, Zhenjiang 212013, China

ABSTRACT: The entire vehicle model of a certain type of car is established, the numerical calculation and analysis on the internal flow field of vehicle model and the aerodynamic noise at the receiving point near the left ear of the driver are carried out based on the large eddy simulation. The distributions of pressure field and velocity in the car are obtained with the different ways of opening the windows and 4 typical operating conditions with different opening degrees. Meanwhile, the frequency domain diagrams of sound pressure level at the reception points near the driver's left ear are acquired. It is derived from the analysis that there is a close relationship between the wind vibration noise in the car and the opening size and opening mode of the car's windows. The wind vibration noise is the smallest when the opening degree of the front window is 1/3. When the opening degrees are same, the wind vibration noise of the rear window is larger than that of the front window. Therefore, the reasonable opening mode and the opening degree of the car's window can effectively control the wind vibration noise. According to the mechanism of wind vibration, the noise reduction method though retrofitting a column is adopted to reduce the noise of the rear window. And the maximum reduction of pressure fluctuation of wind vibration is about 19dB, which improves the passenger ride comfort.

KEYWORDS: Automotive engineering; Wind vibration noise; Numerical calculation; Large eddy simulation.

INTRODUCTION

Noise is an important issue for the automotive industry and researchers [1, 2]. With the effective control of automotive structural noise, the problems of aerodynamic noise gradually highlight when the car is running. The relevant researches show that if the speed of moving vehicle is higher, the flow velocity on the car's surface is larger, the amplitude of fluctuation pressure is greater, the corresponding sound pressure level at each frequency is bigger, the total sound pressure level is greater, and the radiation noise is larger [3]. The opening of automobile's side windows can greatly improve the air flow in the car, but it can cause the aerodynamic noise [4]. The fluctuating pressure produced is easy to cause the driver and the passengers to feel uneasy. From the ride comfort of the driver and passengers, the influence of wind noise must be considered in the design phase of the vehicle. Therefore, there is great practical significance to study the influence of the opening mode and the opening degree of the vehicle's side windows on the wind vibration noise. In 1964, Bodger and Jones firstly carried out the research on the wind vibration noise when the rear windows of bus were open. They pointed out that when the side window was opened, the entire carriage was shaped like a Helmholtz resonant cavity. When the air flowed through the window, the vortex shedding was generated, and the resonance was produced. Three ways to solve the wind vibration noise were put forward from the theoretical aspect [5]. The simulation analysis on the vehicle model which was very close to the real vehicle was carried out through the unstructured grids and the commercial CFD software based on finite element method by Karbon et al. The results obtained were in good agreement with the results of wind tunnel test [6]. The simulation calculation on the airflow noise of the side window of high speed car was completed based on the fluent software by Shen Yugui, etc. The values of fluctuating pressure obtained were basically consistent with the experimental values [7]. The numerical simulation on the characteristics of wind vibration noise under different opening conditions of side window was done through the calculation method of large eddy simulation by Wang Ning, etc. The measures to restrain the wind vibration noise were put forward by using the disturbing flow device [8]. In this paper, the method of large eddy simulation is used to analyze the noise characteristics of the car's side window based on the FLUENT software. The size of wind vibration noise is studied under different opening degrees and opening modes of the side window. And the analytic comparison is carried on. The influences of 4 kinds of different conditions on the sound pressure level near the driver's ears are obtained. And the improvement measures are put forward to the condition with the maximum wind vibration noise [9].

THEORETICAL PRINCIPLE

Aerodynamic Noise Theory

Aerodynamic noise is the result of the interaction between fluid and structure when the fluid flows through the surface of solid. The research method of aerodynamic noise is the "noise analogy" method, which was proposed by Lighthill. It is also known as Lighthill sound analogy method. The Lighthill sound analogy method is based on the mass and momentum conservation equations of fluid mechanics, the wave equation of aerodynamic noise generated due to the turbulent flow in the small scale range surrounded by stationary fluid is derived. The equation expression is as follows [10].

$$\frac{1}{a_0^2} \frac{\partial p'}{\partial t^2} - \nabla^2 p' = \frac{\partial^2}{\partial x_i \partial x_j} T_{ij} \quad (1)$$

Among them,

$$T_{ij} = \rho u_i u_j + (p - p_0 a_0^2) \delta_{ij} - \tau_{ij} \quad (2)$$

Where τ_{ij} is the Lighthill stress tensor, p' is the sound pressure of far field ($p' = p - p_0$), a_0 is the sound velocity of far field, ρ is the air density, u_i and u_j are the velocity components of the flow field in X, Y direction respectively, δ_{ij} is the Kronecker coefficient.

The relationship between the acoustic wave propagation and the characteristics of flow field is established in the Equation (1). It is the most basic equation for solving flow sound.

According to the Kirchhoff method, the Equation (1) is applied to the flow field with the solid boundary by Curle. The Lighthill-Curle equation is derived as follows [11].

$$\begin{aligned} & \left(\frac{1}{a_0^2} \frac{\partial^2}{\partial t^2} - \nabla^2 \right) \left(a_0^2 (\rho - \rho_0) H(f) \right) \\ &= - \frac{\partial}{\partial x_j} \left((\rho v_i v_j + (p - p_0) \delta_{ij} - \sigma_{ij}) \frac{\partial H}{\partial x_j} \right) + \frac{\partial^2}{\partial x_i \partial y_j} (T_{ij} H(f)) \end{aligned} \quad (3)$$

The Equation (3) can effectively describe the problem of fluid sound. But the Curle theory does not apply to the interaction situation between the moving solid boundary and fluid. Based on the Lighthill equation, Ffowcs Williams and Hawkings promoted the Curle theory and made it apply to the effect of the surface of moving object on the sound field. And the more general equation of Williams and Hawkings Ffowcs (FW-H equation) is obtained as follows [12].

$$\begin{aligned} & \left(\frac{1}{a_0^2} \frac{\partial^2}{\partial t^2} - \nabla^2 \right) \left(a_0^2 (\rho - \rho_0) H(f) \right) = \frac{\partial^2}{\partial x_i \partial y_j} (T_{ij} H(f)) \\ & - \frac{\partial}{\partial x_j} \left((\rho v_i (v_j - V_j) + (p - p_0) \delta_{ij} - \sigma_{ij}) \frac{\partial H}{\partial x_j} \right) + \frac{\partial}{\partial t} \left((\rho (v_j - V_j) + \rho_0 V_j) \frac{\partial H}{\partial x_j} \right) \end{aligned} \quad (4)$$

The right side of the Equation (4) can be regarded as the sound source terms. Among them, the first term represents the Lighthill sound source term, which is the quadrupole sound source. The second term is the sound source (force distribution) caused by the surface fluctuating pressure, which is the dipole sound source. The third term represents the sound source (fluid displacement distribution) caused by the acceleration of surface, which is the monopole source. From the Equation (4), it is known that the sound field is formed by the complex interaction between the fluid and the moving object. The sound field is formed by the addition of the quadrupole sound source, the dipole sound source, and the monopole sound source. The Lighthill sound source term exists only outside the surface of moving solid, and it is zero within the surface. And the second and third source terms are generated only on the solid's surface.

Control Equation of Large Eddy Simulation

The large eddy simulation (LES) [13] is a kind of numerical simulation of turbulent flow between the direct numerical simulation (DNS) and the Reynolds average numerical simulation (RANS) [14]. Its basic ideas are to give up the simulation of the eddy motion in the full scale range, but to accurately solve the motion simulation of all the turbulent scales above a certain scale through filtering. Thus, the large scale effect and ordering structure appeared in many processes of non steady state and non equilibrium, which are powerless by the RANS method, can be captured. At the same time, it overcomes the problem of huge calculating cost of the DNS method.

Filtering the N-S equation in the physical space, the governing equations of LES are obtained as follows [15].

$$\frac{\partial}{\partial t}(\rho \bar{u}_i) + \frac{\partial}{\partial x_j}(\rho \bar{u}_i \bar{u}_j) = \frac{\partial}{\partial x_j}(\sigma_{ij}) - \frac{\partial \bar{p}}{\partial x_i} - \frac{\partial \tau_{ij}}{\partial x_j} \quad (5)$$

$$\sigma_{ij} = \left[\mu \left(\frac{\partial \bar{u}_i}{\partial x_j} + \frac{\partial \bar{u}_j}{\partial x_i} \right) \right] - \frac{2}{3} \mu \frac{\partial \bar{u}_i}{\partial x_i} \delta_{ij} \quad (6)$$

In which, \bar{u}_i and \bar{u}_j are the velocity components after filtering, \bar{p} is the pressure after filtering, μ is the viscosity coefficient of turbulence, σ_{ij} is the stress tensor.

ESTABLISHMENT OF MODEL

Establishment of Three Dimensional Model

Because the interior noise of car is the object of study in this paper, the body of car has been simplified without affecting the accuracy of calculation. The four door handles, the front and rear car lights and the antennas were omitted. The car's shape was simplified to a flat surface. The four wheels also were simplified relatively. The length of the car model is 4582 mm, the width is 1795 mm, and the height is 1458 mm. The three dimensional model of whole car established is shown in the Figure 1.

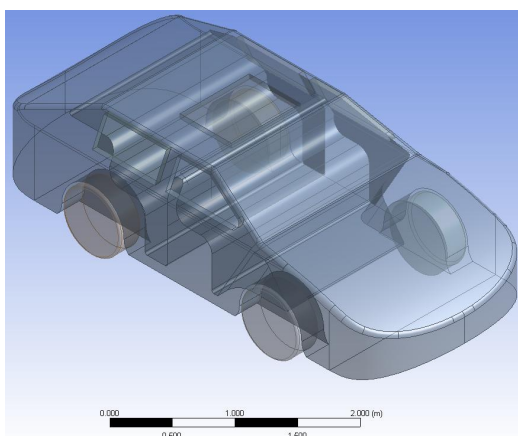


Figure 1. Three dimensional model of whole car.

Determination of Working Conditions

In this paper, the front and rear car windows were opened 1/3 and 2/3 respectively for the analysis of wind vibration noise. The velocity and pressure distributions under different working conditions were compared. And the sound pressure levels near the left ears of driver were compared and analyzed. In order to facilitate the description, the various states were numbered as shown in the Table 1.

Grid Division

The computation domain is a rectangular body that surrounds the car model, as shown in the Figure 2. The distance from the entrance to the front end of car body is about 3 times of the length of car, the distance from the exit to the rear end of car body is about 7 times of the length of car, the height is about 5 times of the height of car, and the width is about 4 times of the length of car.

The shape of car is relatively complex, but the tetrahedral mesh has good adaptability to it, and the capture of geometrical figures is relatively easy. The accuracy of calculation is determined by the size of grid. The smaller the size of grid, the closer to the car's surface, and the calculation results are more accurate. But the calculation time may be very long because the number of grid is too large. Therefore, the mesh of the attachments on the car's surface is denser, and the sparser grid density is used in other places. The grid division of the car model was carried out based on the Gambit software. And the grids were divided as shown in the Figure 3.

Table 1. Opening degrees of car window with four different states.

Opening degrees	Different states
1/3 of front window	Condition 1
2/3 of front window	Condition 2
1/3 of rear window	Condition 3
2/3 of rear window	Condition 4

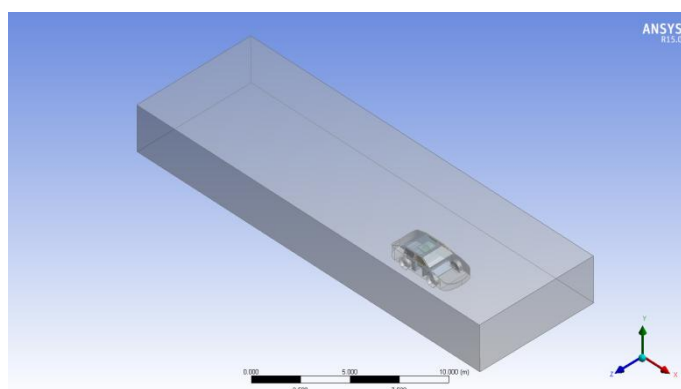


Figure 2. Calculation domain of car model.

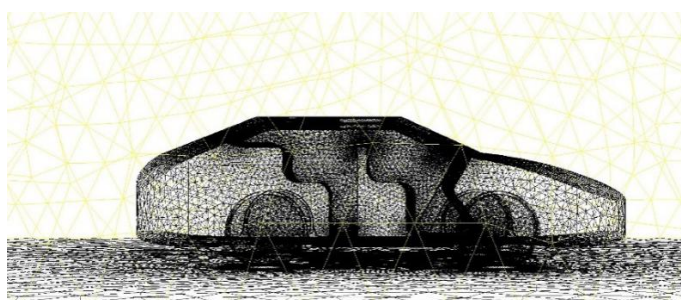


Figure 3. Grid graph of car model.

Setting Boundary Conditions

The most front end of the computational domain was set to the inflow boundary. The uniform speed and accelerating speed were used. The most rear end of the computational domain was set to the outflow boundary, and the flow gradient was zero. The ground was taken as no flow boundary, the boundary condition with non-slip was adopted, and the speed was same as the inlet velocity. The car body was taken as no flow boundary, the boundary condition with non-slip was adopted, and the speed was zero. The slip boundary conditions were used for the left side, right side and the top of car. They were the slip walls of zero shear, and the speed was same as the inlet velocity. The air medium was all in the whole calculation field, the pressure was a standard atmospheric pressure, and the distribution velocity of flow field was the driving speed of car.

SIMULATION ANALYSIS OF AERODYNAMIC NOISE

The transient simulation must be used due to the external unsteady flow of automobile and the fluctuating pressure characteristics. For the transient problems, the simulation of steady state is carried out firstly in general, and then the results of steady state are used as the initial conditions of transient state. First of all, the k-ε turbulence model was adopted to the simulation of model, the inlet speed of computational domain was set to 30 m/s, the export was set as pressure outlet, both sides and top of the computational domain were the sliding surfaces with 30 m/s, and the bottom was a fixed surface.

After many times of convergences of the iterative solutions, the results of steady state were specified as the initial conditions for the transient simulation, and the large eddy simulation (LES) algorithm was used for the transient simulation. The monitoring point was selected near the driver's left ear, and the sampling time was set to 2 s. Since the calculation of flow field from the beginning to the stability need a process and some time, the time domain signals of only 1-2 s were recorded. The time step was set to 0.002 s, the total number of steps was 1000 steps, and 20 times of iterations were done in every time step.

Analysis of Wind Vibration Noise with Different Opening Degrees of Front Window

The calculation and simulation of 'condition 1' and 'condition 2' were carried out. At this time, the front windows were opened 1/3 and 2/3 respectively. The pressure cloud charts, the velocity cloud charts in the car and the sound pressure level curves near the driver's left ear were obtained.



Figure 4. Pressure cloud chart of 'condition 1' in the car.

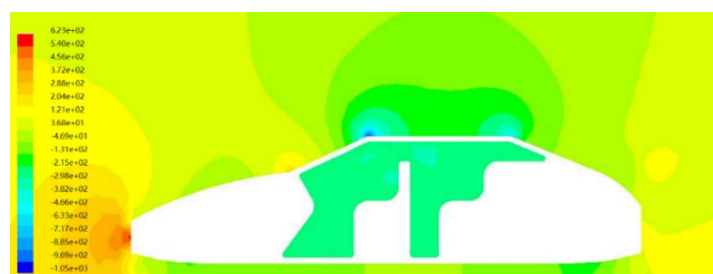


Figure 5. Pressure cloud chart of 'condition 2' in the car.

The pressure cloud charts of the 'condition 1' and the 'condition 2' in the car are shown in the Figures 4 and 5 respectively. It can be known from the pictures above that there is not much difference in the surface pressure distribution of car body between the 'condition 1' and the 'condition 2'. The entire compartment is mainly negative pressure area, and there is obvious positive pressure area only in the front of the car. The pressure fluctuation range of the 'condition 1' in the car is between -474 Pa and -392 Pa. And the pressure fluctuation range of the 'condition 2' in the car is greater than that of the 'condition 1'. From this, we can know that the effect of pressure fluctuation in the car cannot be ignored on the wind buffeting noise.

The velocity cloud charts of the 'condition 1' and the 'condition 2' in the car are shown in the Figures 6 and 7 respectively. It can be known from the pictures above that there is obviously difference in the airflow speed in the car between the 'condition 1' and the 'condition 2'. For the 'condition 1', the airflow velocity only in the upper part of the carriage changes. And for the 'condition 2', the change of airflow velocity appears in the upper part and middle part of the carriage. Therefore, the airflow velocity is also one of important factors affecting the wind vibration noise in the car. The comparative analysis shows that the wind vibration noise of the 'condition 2' is greater than that of the 'condition 1', but the difference is not very big.

The sound pressure level curves of the 'condition 1' and the 'condition 2' near the driver's left ear are shown in the Figures 8 and 9 respectively. The peak value of sound pressure level of the 'condition 1' is about 92 dB, and the peak

value of sound pressure level of the 'condition 2' is about 97 dB. It can be known that the opening degree of the car's window has a noticeable effect on the wind vibration noise.

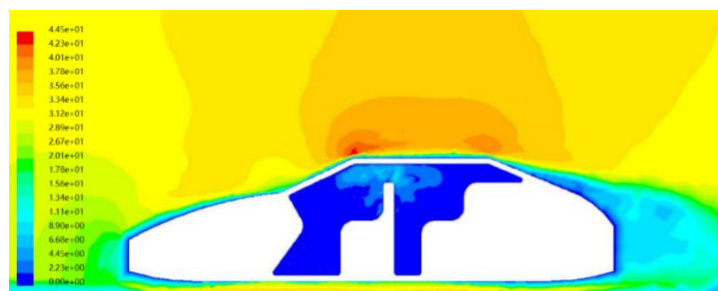


Figure 6. Velocity cloud chart of 'condition 1' in the car.

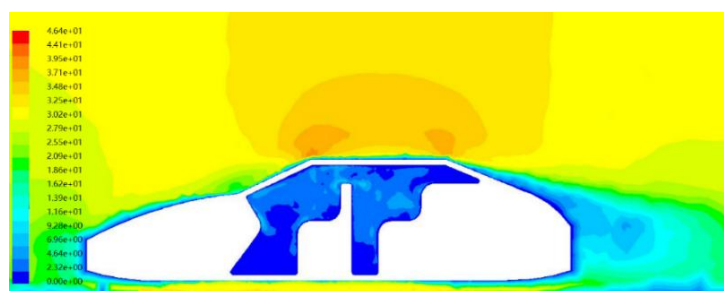


Figure 7. Velocity cloud chart of 'condition 2' in the car.

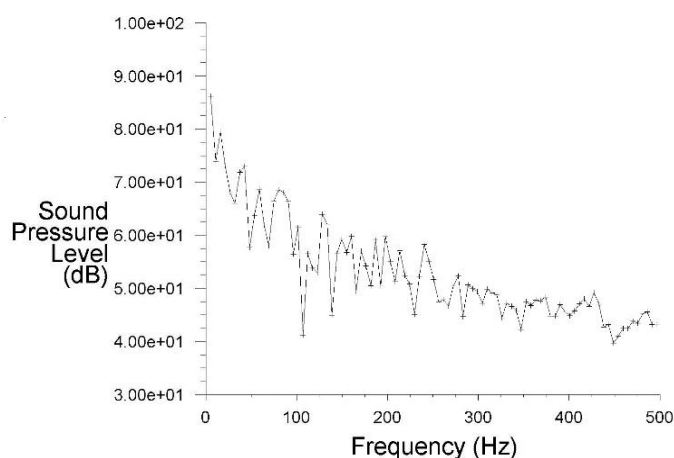


Figure 8. Sound pressure level curve of 'condition 1'.

Analysis of Wind Vibration Noise with Different Opening Degrees of Rear Window

The calculation and simulation of 'condition 3' and 'condition 4' were carried out. At this time, the rear windows were opened 1/3 and 2/3 respectively. The pressure cloud charts, the velocity cloud charts in the car and the sound pressure level curves near the driver's left ear were obtained.

The pressure cloud charts of the 'condition 3' and the 'condition 4' in the car are shown in the Figures 10 and 11 respectively. The overall trends of the internal pressure distribution of the 'condition 3' and the 'condition 4' are similar to the 'condition 1' and the 'condition 2'. The pressure fluctuation range of the 'condition 3' in the car is between -156 Pa and -69.2 Pa. And the pressure fluctuation range of the 'condition 4' in the car is between -214 Pa and -49.8 Pa.

From this, it can be known that the pressure fluctuation range caused by the opening of the rear side window is significantly greater than that caused by the front side window when the opening degrees of the front and rear side windows are same. This is because there is the impediment of rearview mirror near the front side window, which reduces the pressure in the frontal zone.

The velocity cloud charts of the 'condition 3' and the 'condition 4' in the car are shown in the Figures 12 and 13 respectively. It can be known from the pictures above that the air flow in the car of the 'condition 4' is more chaotic than that of the 'condition 3'. For the 'condition 3', the airflow velocity only near the rear seat position changes obviously. And for the 'condition 4', the airflow velocity changes obviously in the whole carriage. Relative to the 'condition 1' and the 'condition 2', the change of airflow velocity caused by the opening of the rear side window is significantly greater than that caused by the opening of the front side window. This is mainly because the laminar boundary layer is formed near the rear windows when the rear window is opened. And the more energy is sent into the carriage, so that the airflow velocity near the rear side window is increased.

The sound pressure level curves of the 'condition 3' and the 'condition 4' near the driver's left ear are shown in the Figures 14 and 15 respectively. The peak value of sound pressure level of the 'condition 3' is about 90 dB, and the peak value of sound pressure level of the 'condition 4' is about 105 dB. Relative to the 'condition 1' and the 'condition 2', the sound pressure level caused by the opening of the rear side window is significantly greater than that caused by the opening of the front side window. This is because the pressure fluctuation range is relatively large in the car when the rear window is opened, which increases the vibration energy inside the carriage to make the sound pressure level near the driver's ear rise.

CONTROL OF WIND VIBRATION NOISE OF REAR SIDE WINDOW

From the above analysis, it can be known that the laminar boundary layer is formed near the rear windows when the rear window is opened, the more energy is sent into the carriage to make the wind vibration noise increase. Therefore, the rear window is the key of optimization of the wind vibration noise. In this paper, the 'condition 4' with the maximum wind vibration noise is selected as the research object. A column is added to the rear window for reducing the wind vibration noise. The improved model of whole car is shown in the Figure 16.

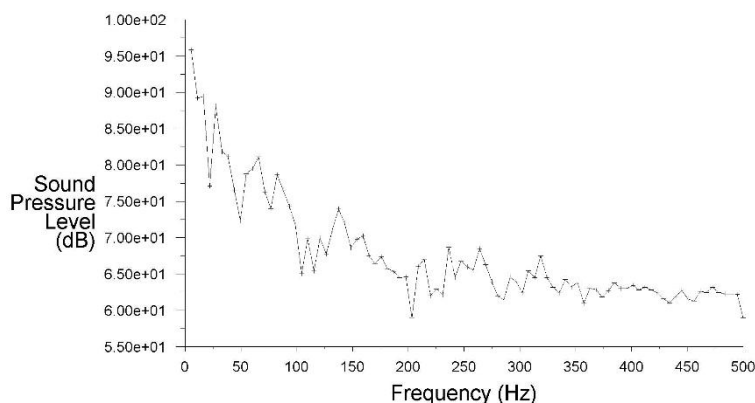


Figure 9. Sound pressure level curve of 'condition 2'.



Figure 10. Pressure cloud chart of 'condition 3' in the car.



Figure 11. Pressure cloud chart of 'condition 4' in the car.



Figure 12. Velocity cloud chart of 'condition 3' in the car.

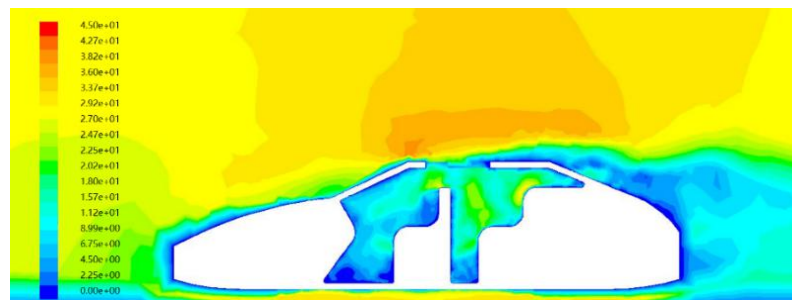


Figure 13. Velocity cloud chart of 'condition 4' in the car.

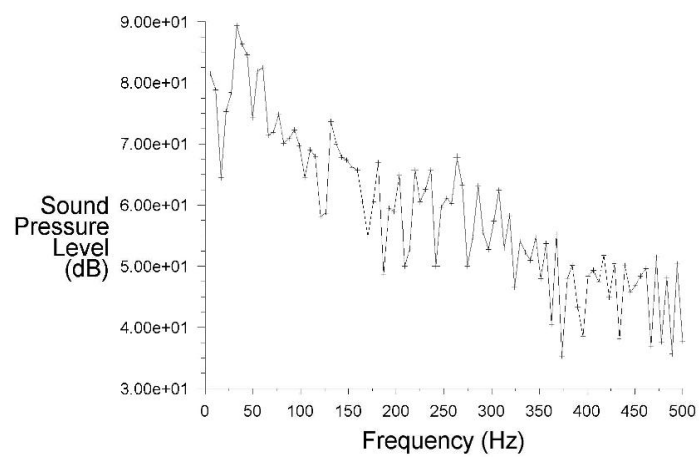


Figure 14. Sound pressure level curve of 'condition 3'.

Figure 15. Sound pressure level curve of 'condition 4'.

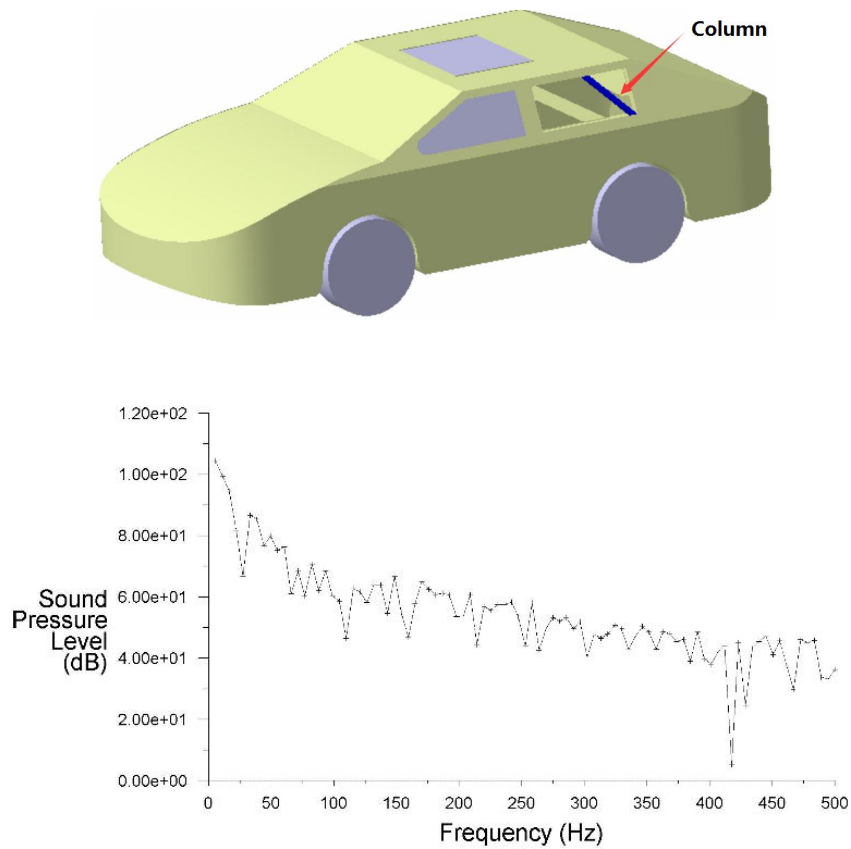


Figure 16. Improved model of whole car.

The analysis of wind vibration noise of the improved car was carried out. The pressure distribution obtained in the car is shown in the Figure 17. The velocity distribution obtained in the car is shown in the Figure 18. And the sound pressure distribution in the car is shown in the Figure 19.



Figure 17. Pressure cloud chart of 'condition 4' in the improved car.

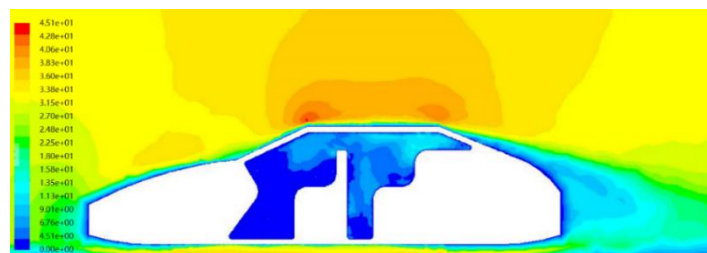


Figure 18. Velocity cloud chart of 'condition 4' in the improved car.

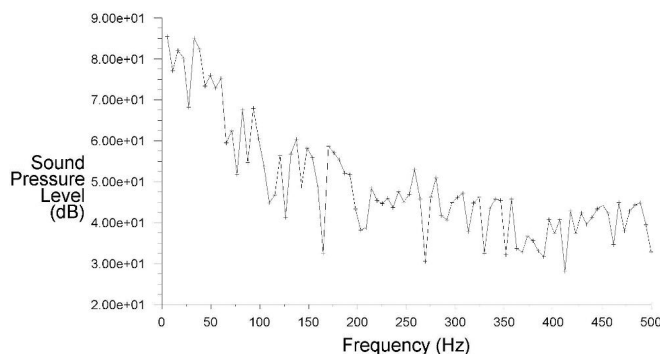


Figure 19. Sound pressure level curve of 'condition 4' in the improved car.

It can be known from the Figures 17, 18 and 19 that the pressure fluctuation range of the 'condition 4' in the improved car is between -246 Pa and -156 Pa, the airflow velocity has a significant decline in the improved car and its maximum value is only about 18m/s, the peak value of sound pressure level near the driver's left ear is about 86 dB and its value is decreased by about 19 dB.

CONCLUSIONS

Through the large eddy simulation method, the surface flow pattern, fluctuating pressure and the sound pressure near the driver's ear were calculated to the different opening ways and opening degrees. The following conclusions are drawn:

- (1) The greater the opening degree of car's window, the greater the wind vibration noise.
- (2) When the opening degrees of car's windows are same, the wind vibration noise caused by the rear window is larger than that of the front window.
- (3) The wind vibration noise near the rear window can be controlled effectively through adding a column in the rear window. The peak value of sound pressure level is decreased by about 19dB.

CONFLICT OF INTEREST

The authors confirm that this article content has no conflict of interest.

ACKNOWLEDGEMENTS

This research is supported by the National Natural Science Foundation of China (51575238), the Jiangsu Province Ordinary University Graduate Research and Innovation Project (KYLX_1024), and the Basic and Applied Basic Research Fund Project of Jiangsu University of Technology (KYY14009).

REFERENCES

- [1] G. Q. Wu, Y. Sheng, and Y. Fang, "Coupled acoustic-structural finite element analysis of vehicle interior noise based on acoustic sensitivity", *Journal of Mechanical Engineering*, vol. 45, no. 3, pp. 222-228, 2009.
- [2] J. Q. Gao, X. X. Jin, G. D. Lu, et al, "Simulation study on car interior noise based on SEA", *Automobile Technology*, no. 6, pp. 23-27, 2009.
- [3] T. Lan, N. Kang, H. Zheng, and C. A. Hu, "Study on the aerodynamic noise of a fastback car with rear view mirrors in uniform motion and accelerated motion", *Journal of Aerospace power*, vol. 24, no. 1, pp. 116-121, 2009.
- [4] J. P. Chen, Z. P. Sun, and X. C. Que, "Numerical simulation of airflow and temperature in the car with passenger", *Automotive Engineering*, vol. 21, no. 5, pp. 309-3131, 1999.
- [5] W. K. Bodger and C. M. Jones, "Aerodynamic wind thrombin passenger cars", SAE Technical Paper 640797, 1964.
- [6] K. J. Karbon, S. Kumarasamy, and R. Singh, "Applications and issues in automotive computational aeroacoustics", Canada: Proceedings of the 10th Annual Conference of the CFD Society of Canada, Taylor & Francis, 2002.

- [7] Y. G. Shen, S. L. Lu, and X. Meng, "Simulation on aerodynamic noise of automobile's side window at high speed", *Machinery Design & Manufacture*, no. 7, pp. 125-127, 2012.
- [8] N. Wang, Z. Q. Gu, S. C. Liu, G. P. Dong, and L. G. Liu, "Wind buffeting noise analysis and control for high-speed vehicle side-windows", *Journal of Aerospace Power*, vol. 28, no. 1, pp. 112-119, 2013.
- [9] J. Wang, Z. L. Liu, and Y. Chen, "Comparative analysis of economic efficiency of grain storage by solar absorption refrigeration", *AISS: Advances in Information Sciences and Service Sciences*, vol. 4, no. 14, pp. 341-348, 2012. doi: 10.4156/AISS.
- [10] S. D. Sovani and C. Kuo-Huey, "Aero acoustics of an automotive a-pillar raingutter: A numerical study with the flowcs-williams hawkins method", *SAE paper*, 2005-01-2492.
- [11] V. Kannan, D. S. Sandeep, and S. Greeley Dave, "3D computational aero acoustics simulation of air intake-induced whistles", *Bosch Inc*, 2004.
- [12] W. Tian, "Numerical simulation and analysis of automobile wind noise", Nanjing University of Science and Technology, 2006.
- [13] D. Feng, X. Wang, F. Jiang, et al, "Large eddy simulation of darpa suboff for $Re= 2.65 \times 10^7$ ", *Journal of Coastal Research*, vol. 73, no. sp1, pp. 687-691, 2015.
- [14] W. Rodi, "DNS and LES of some engineering flows", *Fluid Dynamics Research*, vol. 38, pp. 145-173, 2006.
- [15] H. J. Zhu, *Practical guide of flow field analysis based on FLUENT 15.0*. Beijing: People's Posts and Telecommunications Press, 2014.